AIP Applied Physics Letters

# Surface passivation of c-Si by atmospheric pressure chemical vapor deposition of Al2O3

Lachlan E. Black and Keith R. McIntosh

Citation: Applied Physics Letters **100**, 202107 (2012); doi: 10.1063/1.4718596
View online: http://dx.doi.org/10.1063/1.4718596
View Table of Contents: http://scitation.aip.org/content/aip/journal/apl/100/20?ver=pdfcov
Published by the AIP Publishing

# Surface passivation of c-Si by atmospheric pressure chemical vapor deposition of $Al_2O_3$

Lachlan E. Black[1,a)] and Keith R. McIntosh[2]
[1]*Centre for Sustainable Energy Systems, College of Engineering and Computer Science, Australian National University, Canberra ACT 0200, Australia*
[2]*PV Lighthouse, Coledale NSW 2515, Australia*

(Received 18 November 2011; accepted 29 April 2012; published online 16 May 2012)

Atmospheric pressure chemical vapor deposition of $Al_2O_3$ is shown to provide excellent passivation of crystalline silicon surfaces. Surface passivation, permittivity, and refractive index are investigated before and after annealing for deposition temperatures between 330 and 520 °C. Deposition temperatures >440 °C result in the best passivation, due to both a large negative fixed charge density ($\sim 2 \times 10^{12}\,cm^{-2}$) and a relatively low interface defect density ($\sim 1 \times 10^{11}\,eV^{-1}\,cm^{-2}$), with or without an anneal. The influence of deposition temperature on film properties is found to persist after subsequent heat treatment. Correlations between surface passivation properties and the permittivity are discussed. © *2012 American Institute of Physics*. [http://dx.doi.org/10.1063/1.4718596]

Silicon surface passivation by aluminum oxide ($Al_2O_3$) is currently a subject of significant research within the photovoltaic industry. The distinctive feature of this material is its high density of negative fixed charge, which combined with a relatively low interface defect density has been shown to provide excellent passivation of silicon surfaces.[1–10] In particular, it is able to effectively passivate both diffused and undiffused p-type surfaces, a task for which conventional positively charged silicon nitride ($SiN_x$) passivation layers have generally been found to be unsuited[11,12] (although it should be noted that good passivation of boron emitters with $SiN_x$ has recently been observed in some cases following a firing step[13]). An effective means of passivating such surfaces is necessary both to overcome efficiency limitations imposed by the use of conventional Al-diffused "back surface fields," and to enable the adoption of cells based on n-type silicon, with its attendant advantages.[14]

$Al_2O_3$ for surface passivation has to date been mostly deposited by conventional atomic layer deposition (ALD), a technique that allows for very fine control of film thickness and a high degree of conformality, but which does not provide the high throughput necessary for application in the photovoltaic industry. Recent work has, therefore, focused on alternative high-throughput deposition techniques, such as plasma-enhanced chemical vapor deposition (PECVD),[8–10,15,16] reactive sputtering,[10,17] and high-rate spatial ALD.[10,18,19] Promising results have been achieved with all of these methods, although sputtered films still lag behind PECVD and ALD in terms of surface passivation. Other deposition techniques such as sol-gel[20,21] and evaporation[22] have so far shown only marginal passivation potential. It is evident that passivation depends sensitively on interfacial rather than bulk film properties,[23] and that these may be strongly dependent on the method used to synthesize the films. Even for techniques based on similar principles, such as ALD and PECVD, differences in activation method (thermal or plasma), deposition regime (temperature and pressure, self-limiting, or continuous reactions), and chemistry (precursors) may result in fundamentally different film structures and properties, and passivation may only be achieved under a limited range of process conditions.

Despite the interest in high-throughput alternatives to ALD, one comparatively simple high-throughput technique has so far been neglected, namely atmospheric pressure chemical vapor deposition (APCVD). This is ironic, given that APCVD was used in the first work on surface passivation with $Al_2O_3$, that of Hezel and Jaeger in 1989.[24] While they achieved promising results, their work was not followed up until 2006, and then with ALD.[5,6] In this paper, we investigate the surface recombination velocity, interface defect density, and fixed charge of APCVD $Al_2O_3$ on silicon surfaces, as a function of deposition temperature and annealing, using photoconductance and capacitance-voltage (C-V) techniques. It is found that $Al_2O_3$ deposited by APCVD can provide excellent surface passivation of crystalline silicon surfaces, comparable to the best results of PECVD and ALD. Furthermore, we demonstrate the dependence of passivation properties on deposition temperature and subsequent annealing and show how these properties are correlated with the permittivity of the films.

$Al_2O_3$ films were deposited using an inline APCVD belt furnace system manufactured by SierraTherm Production Furnaces Inc. A detailed description of this system is given elsewhere.[25] Triethyldialuminum tri-(*sec*-butoxide) (TEDA-TSB)[26] was used as the chemical precursor. Like trimethylaluminum (TMA), the precursor generally used in ALD and PECVD deposition of $Al_2O_3$, this material forms a low-viscosity liquid at room temperature, but unlike TMA it has the practical advantage of being non-pyrophoric and, therefore, easier to handle. TEDA-TSB was reacted with water vapor at substrate temperatures between 330 and 520 °C to form $Al_2O_3$. Substrates were passed under the injector head on a moving belt at a speed of 12 in. per minute. All films deposited at a given temperature were deposited in the same run. Post-deposition annealing was performed in a quartz tube furnace under various ambients at either 400 or 425 °C.

a)Electronic mail: lachlan.black@anu.edu.au.

 

Lifetime measurements were performed on 325 $\mu$m thick 0.8 Ω cm p-type ⟨100⟩ FZ-Si wafers. The wafers were etched in TMAH to remove saw damage, cleaned by the RCA (Radio Corporation of America) procedure, and diffused with phosphorus to getter iron impurities. The wafers were then etched in HCl to remove the phosphorus diffusions, cleaned by the RCA procedure, and given an HF dip and de-ionized (DI) water rinse to remove the native oxide just prior to the deposition of APCVD $Al_2O_3$. The $Al_2O_3$ was deposited on the front surface and then the rear surface immediately after.

The samples prepared for capacitance-voltage measurements were fabricated from 8 Ω cm p-type ⟨100⟩ Cz-Si wafers and 1 Ω cm n-type ⟨100⟩ FZ-Si wafers. The front surfaces of these wafers were polished. The wafers were cleaned by the RCA procedure, including an HF dip and DI water rinse, just prior to the deposition of APCVD $Al_2O_3$. Al dot contacts were thermally evaporated on the front side through a shadow mask, while GaIn paste was applied to the rear side to form an ohmic contact. For annealed samples, annealing occurred prior to contact deposition.

Carrier lifetime was measured using a Sinton Labs WCT-120 photoconductance tool operated in either transient or generalized quasi-steady-state mode. The upper limit of the effective surface recombination velocity $S_{eff,UL}$ was calculated according to

$$S_{eff,UL} = \frac{W}{2}\left[\frac{1}{\tau_{eff}} - \frac{1}{\tau_{bulk,\text{intrinsic}}}\right],$$

where $W$ is the sample thickness, $\tau_{eff}$ is the measured effective minority carrier lifetime at an excess carrier concentration of $10^{15}\,\text{cm}^{-3}$, and $\tau_{bulk,intrinsic}$ is the Auger-limited intrinsic bulk lifetime determined using the parameterization of Kerr and Cuevas.[27]

High frequency and quasi-static capacitance-voltage measurements were performed using an HP 4284 A Precision LCR Meter and HP 4140B Picoammeter/DC Voltage Source. Capacitance measurements were corrected for parasitic series resistance and inductance, leakage currents, and dielectric dispersion. Gate area was determined on an individual basis using optical microscopy. The method of Ghibaudo *et al.*[28] was used to determine the insulator capacitance, while the flatband voltage was determined from the offset of the measured and ideal high-frequency curves in depletion, after correction for interface trap stretchout.[29] The midgap interface defect density $D_{it}$ was extracted using the combined high-frequency/quasi-static capacitance method.[30] Fixed charge $Q_f$ was calculated by assuming all charge to be located at the Si–$Al_2O_3$ interface, using work function values of $W_{Al} = 4.23$ V and $W_{Si(100)} = 4.71$ V for the aluminum gate and silicon substrate, respectively.[31] A more detailed description of the analysis procedure used is in preparation for a separate publication.

The $Al_2O_3$ refractive index was determined as a function of deposition temperature by fitting a combination of polarized multi-angle reflectance and fixed-angle spectral ellipsometry measurements with optical modeling software. Film thickness for individual capacitance-voltage samples was then determined by fitting normal incidence spectral reflection measurements (Filmetrics F20 Thin Film Measurement System) with the extracted values of $n$ and $k$. The reported values are averages derived from multiple measurements over the area of each sample. Standard deviation was always less than 5% and generally less than 3%. The dielectric constant $\kappa$ was calculated from this thickness and the average insulator capacitance determined from both high-frequency (1 MHz) and quasi-static C-V measurements on the same samples.

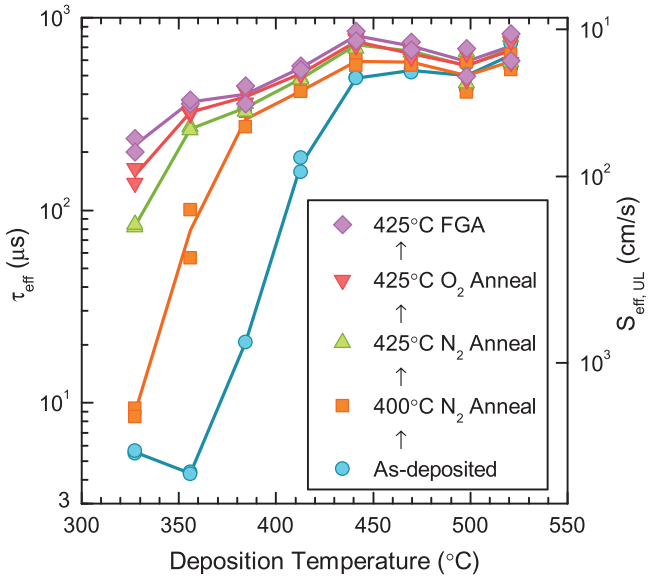


FIG. 1. $\tau_{eff}$ and $S_{eff,UL}$ as a function of $Al_2O_3$ deposition temperature. Values are presented as-deposited and after various successive 30 min post-deposition anneals. Results from two samples, taken from different wafers, are shown at each deposition temperature and annealing step. Lines are plotted between mean values at each temperature.

Figure 1 shows effective minority carrier lifetime as a function of deposition temperature prior to annealing (blue circles) and after successive anneals. The lifetime increases markedly with increasing deposition temperature over the range 330–440 °C, and plateaus at 440–520 °C. Subsequent annealing results in increased lifetime, with the relative increase being greater for lower deposition temperatures. Whether the annealing ambient is important is unclear from this exploratory study and will be the subject of further work. It is interesting to note that the influence of deposition temperature on lifetime is reduced, but not eliminated by subsequent anneals. This suggests that a significantly larger thermal budget is needed to achieve the same level of surface passivation when applied after rather than during deposition.

A minimum $S_{eff,UL}$ of 10 cm/s was achieved at a deposition temperature of 440 °C, after annealing. This is the best value of surface recombination velocity reported to date for $Al_2O_3$ on such heavily doped substrates. It is comparable to the best values reported for $Al_2O_3$ from thermal and spatial ALD (both 4 cm/s) and PECVD (5 cm/s) for less heavily doped 1.3 Ω cm p-type samples,[10] and much better than the value of 55 cm/s reported for sputtered films on the same substrates.[17] For comparison, $S_{eff,UL}$ values of 5 cm/s and 12 cm/s have been reported as exemplary values for alnealed $SiO_2$ and $SiN_x$, respectively, on 1 Ω cm p-type substrates.[32,33] We note that we have measured lower values of $S_{eff,UL}$ than those reported here with the same APCVD $Al_2O_3$

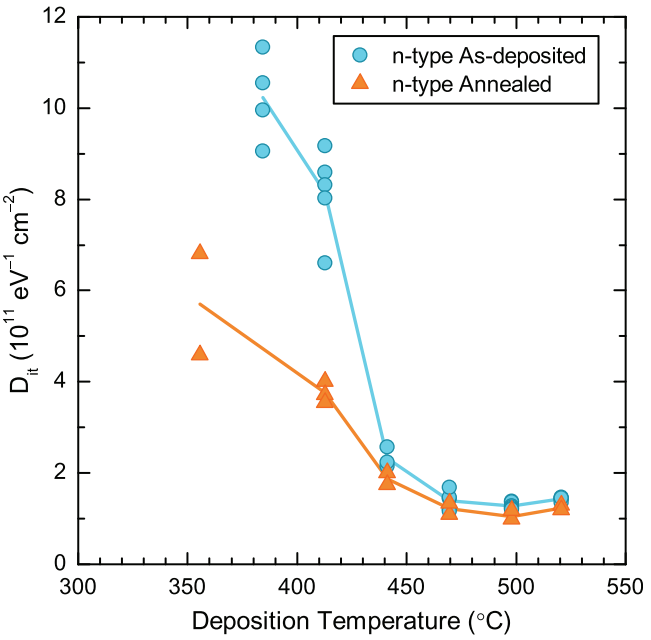


FIG. 2. Midgap interface defect density $D_{it}$ as a function of film deposition temperature, both as-deposited and after annealing at 400 °C in $N_2$ for 30 min. As-deposited and annealed values are for separate samples with films deposited in the same run. Lines are plotted between mean values at each temperature.

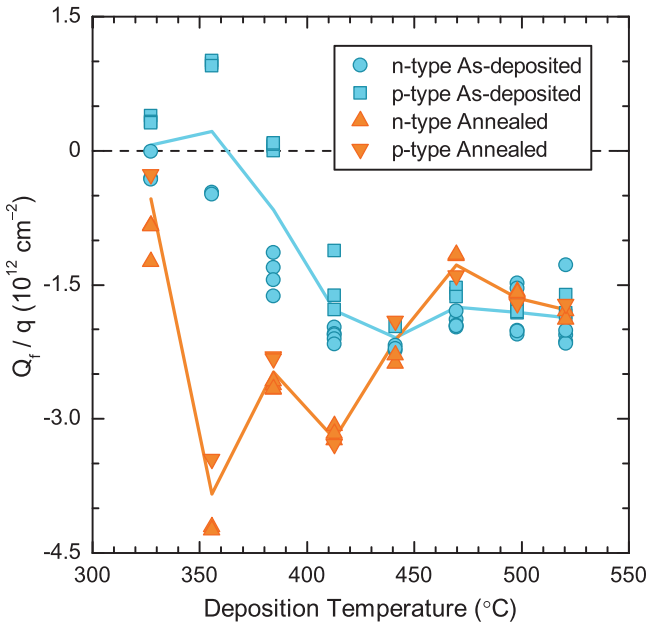


FIG. 3. Fixed charge density $Q_f/q$ as a function of film deposition temperature, both as-deposited and after annealing at 400 °C in $N_2$ for 30 min. Values are shown both for p and n-type samples. As-deposited and annealed values are for separate samples with films deposited in the same run. Lines are plotted between mean values for p- and n-type samples at each temperature.

films on different substrates, and these are reported elsewhere,[25] where they are compared with the results of other techniques.

The C-V measurements show how the deposition temperature and the post-deposition anneal influence the interface states and the charge density, which in turn determine surface recombination. Figure 2 shows the interface defect density and Figure 3 the fixed charge density for films deposited at temperatures between 330–520 °C, both before and after annealing in $N_2$ at 400 °C for 30 min. Interface defect density decreases with increasing deposition temperature, falling sharply between 410–440 °C and leveling out at $\sim 1.4 \times 10^{11}\,eV^{-1}\,cm^{-2}$ above 470 °C. Annealing results in a reduction in defect density across all deposition temperatures, although $D_{it}$ remains higher for films deposited at lower temperatures. For films deposited at temperatures above 440 °C, annealing has only a minor effect on $D_{it}$, reducing it to $\sim 1.2 \times 10^{11}\,eV^{-1}\,cm^{-2}$ for temperatures above 470 °C.

These trends for $D_{it}$ correlate directly to those for $S_{eff,UL}$, but the passivation is also influenced by the charge density in the films. Figure 3 shows that the charge density is zero, within error, for films deposited at 355 °C or below, and increases sharply at higher temperatures, appearing to plateau at $-1.8$ to $-2.2 \times 10^{12}\,cm^{-2}$ above 410 °C. Following annealing, the trend is reversed, with films deposited at lower temperatures having higher charge, with the apparent exception of the films deposited at the lowest temperature, 330 °C. Above 440 °C, charge is actually reduced somewhat by annealing. It is interesting to note that the value of $Q_f$ is very similar for substrates of both polarities when $D_{it}$ is small. This allows us to be confident in the work function values used in the extraction and indicates that the charge in the film is independent of the substrate doping. The large difference in apparent $Q_f$ at flatband for n- and p-type samples at lower temperatures is consistent with the effect of interface trapped charge $Q_{it}$, which scales directly with $D_{it}$ and will most likely be positive for p-type samples and negative for n-type.[29] The true value of $Q_f$ at these temperatures will, therefore, be somewhere between the measured p- and n-type values.

The extracted values of $D_{it}$ and charge compare closely to those reported in the literature for ALD and PECVD, which are typically on the order of $\sim 1 \times 10^{11}\,eV^{-1}\,cm^{-2}$ for $D_{it}$ and $10^{12}$–$10^{13}\,cm^{-2}$ for charge.[1–3,7–9,15,16,34] They are similar to the results reported recently by Dingemans *et al.*[7] of $D_{it} = 1 \times 10^{11}\,eV^{-1}$, and $Q_f/q = -2.4 \times 10^{12}\,cm^{-2}$ for thermal ALD films annealed at the same temperature. Notably, however, such excellent values are achieved here even without any post-deposition annealing. The values of $D_{it}$ are the lowest reported for as-deposited $Al_2O_3$. Indeed, the lifetime results confirm that there is little need to anneal the films to gain excellent surface passivation, so long as deposition occurs above 440 °C.

It is desirable to link changes in $D_{it}$ and $Q_f$ to structural changes in the film, and these may be elucidated by studying other film properties. Figure 4 shows $Al_2O_3$ film thickness, refractive index $n$, and both high-frequency and static dielectric constant $\kappa$ as a function of deposition temperature before and after annealing. Film thickness varies between 13 and 25 nm and is generally thicker for lower temperatures. No change in thickness is observed with annealing. Previous studies have observed no thickness dependence of $Al_2O_3$ passivation for thicknesses $>\sim 10$ nm, so this variation is unlikely to be the cause of the differences in passivation properties observed here.[23] Refractive index is practically constant with temperature, with an average value of $n = 1.62$ at a wavelength of 632 nm. Since refractive index is related

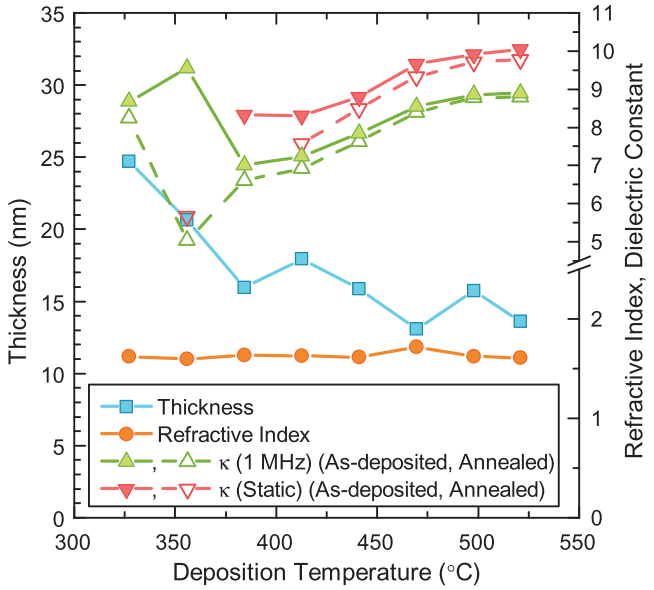


FIG. 4. $Al_2O_3$ film thickness, refractive index $n$ at a wavelength of 632 nm, and both high-frequency (1 MHz) and static dielectric constants $\kappa$ as a function of $Al_2O_3$ deposition temperature. The dielectric constant is shown before and after annealing. For the thickness and refractive index, the measurement error is generally smaller than the symbol size. The relative error for $\kappa$ is estimated to be approximately 3%, most of which is due to systematic error in the extraction of the insulator capacitance.

to density, this suggests that density also does not vary significantly with temperature. The reduction in thickness at higher temperatures is, therefore, due to a lower deposition rate, which is consistent with the presence of parasitic gas-phase reactions.[35] In contrast, the dielectric constant varies strongly with deposition temperature, increasing from a minimum of 7.0 at 385 °C to 8.9 at 520 °C (taking the values at 1 MHz). This is most likely due to a gradual change in the bonding configuration within the amorphous films, resulting in a larger contribution of lattice polarization.[36] We note that this increase in permittivity is correlated with the reduction of $D_{it}$. The sharp increase of the dielectric constant below 355 °C is likely to be related to significantly increased hydrogen incorporation in these films (probably in the form of OH groups),[37] resulting in a strong dipolar contribution.[38] This transition appears to coincide with the appearance of significant negative charge in the films. It is notable that the magnitude of the post-annealing reduction in permittivity of the films deposited at the lowest two temperatures is correlated with the change in fixed charge density of the same samples (Figure 3). This could be explained if desorption of hydrogen during annealing (and consequent reduction of the dipolar contribution to permittivity) is linked to the formation of negative charge centers (possibly oxygen interstitials[39]). The reason why a smaller reduction is observed for the lowest temperature film is unclear, though it is possible that its greater thickness may restrict hydrogen desorption. Further investigation is needed to establish these relationships more firmly.

Our results show that excellent passivation can be achieved with $Al_2O_3$ using a relatively simple deposition technique, APCVD. It is evident that the optimal deposition temperature for the precursors used lies at 440–520 °C, where an $S_{eff,UL}$ of 13 cm/s was attained before annealing and 10 cm/s after. It was shown that this temperature provides the lowest $D_{it}$, both before and after annealing. It was also shown that there is little charge within the films when deposited at <355 °C and that it increases with temperature to up to $2.2 \times 10^{12}$ cm$^{-2}$ above 410 °C, but increases above this value for lower temperatures after the anneal. $S_{eff,UL}$, $D_{it}$ and charge were found to have a dependence on deposition temperature that persisted even after annealing. Changes in these values were observed to be linked to variations of the permittivity, suggesting that the reduction of $D_{it}$ at higher temperatures is linked to lattice restructuring in the film, and that there is a relationship between the generation of negative charge centers and the reduction of permittivity during deposition and annealing.

The authors would like to thank Kenneth M. Provancha and James N. Cotsell for their invaluable technical assistance.

[1]B. Hoex, S. B. S. Heil, E. Langereis, M. C. M. van de Sanden, and W. M. M. Kessels, Appl. Phys. Lett. **89**, 042112 (2006).
[2]G. Agostinelli, A. Delabie, P. Vitanov, Z. Alexieva, H. F. W. Dekkers, S. De Wolf, and G. Beaucarne, Sol. Energy Mater. Sol. Cells **90**, 3438 (2006).
[3]B. Hoex, J. Schmidt, P. Pohl, M. C. M. van de Sanden, and W. M. M. Kessels, J. Appl. Phys. **104**, 044903 (2008).
[4]G. Dingemans, P. Engelhart, R. Seguin, F. Einsele, B. Hoex, M. C. M. van de Sanden, and W. M. M. Kessels, J. Appl. Phys **106**, 114907 (2009).
[5]G. Dingemans, R. Seguin, P. Engelhart, M. C. M. van de Sanden, and W. M. M. Kessels, Phys. Status Solidi RRL **4**, 10 (2010).
[6]J. Schmidt, B. Veith, F. Werner, D. Zielke, and R. Brendel, in *Proceedings of the 35th IEEE PVSC, Honolulu, USA, 20–25 June 2010* (IEEE, 2010), pp. 885–890.
[7]G. Dingemans, N. M. Terlinden, D. Pierreux, H. B. Profijt, M. C. M. van de Sanden, and W. M. M. Kessels, Electrochem. Solid State **14**, H1 (2011).
[8]G. Dingemans, M. C. M. van de Sanden, and W. M. M. Kessels, Electrochem. Solid State **13**, H76 (2010).
[9]G. Dingemans, P. Engelhart, R. Seguin, M. M. Mandoc, M. C. M. van de Sanden, and W. M. M. Kessels, in *Proceedings of the 35th IEEE PVSC, Honolulu, USA, 20–25 June 2010* (IEEE, 2010), pp. 3118–3121.
[10]J. Schmidt, F. Werner, B. Veith, D. Zielke, R. Bock, V. Tiba, P. Poodt, F. Roozeboom, A. Li, A. Cuevas, and R. Brendel, in *Proceedings of the 25th EUPVSEC, Valencia, Spain, 6–10 September 2010* (WIP, 2010), pp. 1130–1133.
[11]S. Dauwe, L. Mittelstädt, A. Metz, and R. Hezel, Prog. Photovolt: Res. Appl. **10**, 271 (2002).
[12]M. J. Kerr, Ph.D. dissertation, Australian National University, Canberra, 2002.
[13]F. Chen, I. Romijn, A. Weeber, J. Tan, B. Hallam, and J. Cotter, in *Proceedings of the 22nd EUPVSEC, Milan, Italy, 3–7 September 2007* (WIP, 2007), pp. 1326–1331.
[14]D. Macdonald and L. J. Geerligs, Appl. Phys. Lett. **85**, 4061 (2004).
[15]P. Saint-Cast, D. Kania, M. Hofmann, J. Benick, J. Rentsch, and R. Preu, Appl. Phys. Lett. **95**, 151502 (2009).
[16]S. Miyajima, J. Irikawa, A. Yamada, and M. Konagai, Appl. Phys. Express **3**, 012301 (2010).
[17]T. T. Li and A. Cuevas, Phys. Status Solidi RRL **3**, 160 (2009).
[18]P. Poodt, A. Lankhorst, F. Roozeboom, K. Spee, D. Maas, and A. Vermeer, Adv. Mater. **22**, 3564 (2010).
[19]G. Dingemans and W. M. M. Kessels, in *Proceedings of the 25th EUPVSEC, Valencia, Spain, 6–10 September 2010* (WIP, 2010), pp. 1083–1090.
[20]P. Vitanov, A. Harizanova, T. Ivanova, and T. Dimitrova, Thin Solid Films **517**, 6327 (2009).
[21]H. Xiao, C. Zhou, X. Cao, W. Wang, L. Zhao, H. Li, and H. Diao, Chin. Phys. Lett. **26**, 088102 (2009).
[22]M. Y. Seo, E. N. Cho, C. E. Kim, P. Moon, and I. Yun, in *Proceedings of the 3rd INEC, Hong Kong, China, 3–8 January 2010* (IEEE, 2010), pp. 238–239.

[23]F. Werner, B. Veith, D. Zielke, L. Kühnemund, C. Tegenkamp, M. Seibt, R. Brendel, and J. Schmidt, J. Appl. Phys. **109**, 113701 (2011).
[24]R. Hezel and K. Jaeger, J. Electrochem. Soc. **136**, 518 (1989).
[25]L. E. Black, K. M. Provancha, and K. R. McIntosh, in *Proceedings of the. 26th EUPVSEC, Hamburg, Germany, 5–9 September 2011* (WIP, 2011), pp. 1120–1124.
[26]R. G. Gordon, K. Kramer, and X. Liu, Mater. Res. Soc. Symp. Proc. **446**, 383 (1997).
[27]M. Kerr and A. Cuevas, J. Appl. Phys. **91**, 2473 (2002).
[28]G. Ghibaudo, S. Bruyère, T. Devoivre, B. DeSalvo, and E. Vincent, IEEE Trans. Semicond. Manuf. **13**, 152 (2000).
[29]E. H. Nicollian and J. R. Brews, *MOS (Metal Oxide Semiconductor) Physics and Technology* (Wiley, New York, 1982), pp. 477–486.
[30]R. Castagné and A. Vappaille, Surf. Sci. **28**, 157 (1971).
[31]H. Kawano, Prog. Surf. Sci. **83**, 1 (2008).
[32]M. J. Kerr and A. Cuevas, Semicond. Sci. Technol. **17**, 35 (2002).
[33]M. J. Kerr and A. Cuevas, Semicond. Sci. Technol. **17**, 166 (2002).
[34]B. Hoex, J. J. H. Gielis, M. C. M. van de Sanden, and W. M. M. Kessels, J. Appl. Phys. **104**, 113703 (2008).
[35]E. J. Kim and W. N. Gill, J. Cryst. Growth **140**, 315 (1994).
[36]H. Momida, T. Hamada, and Y. Takagi, Phys. Rev. **73**, 054108 (2006).
[37]A. N. Gleizes, C. Vahlas, M. Sovar, D. Samélor, and M. Lafont, Chem. Vap. Deposition **13**, 23 (2007).
[38]K. Murase, Jpn. J. Appl. Phys. **33**, 1385 (1994).
[39]J. R. Weber, A. Janotti, and C. G. Van de Walle, J. Appl. Phys. **109**, 033715 (2011).